AD-A103 731 COLD REGIONS RESEARCH AND ENGINEERING LAB HANOVER NH F/G 8/12
INVESTIGATION OF THE ACOUSTIC EMISSION AND DEFORMATION RESPONSE--ETC(U)
APR 81 P C XIROUCHAKIS, M CHAPLIN
UNCLASSIFIED CRREL-81-6 NL

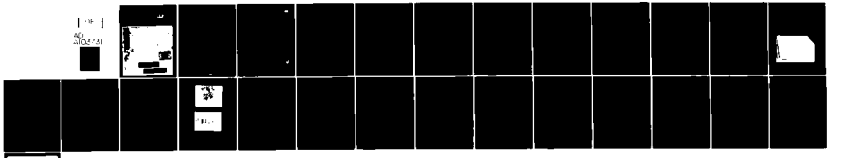

END
DATE FILMED
10 81
DTIC

CRREL

REPORT 81-6

LEVEL II

12

Investigation of the acoustic emission and deformation response of finite ice plates

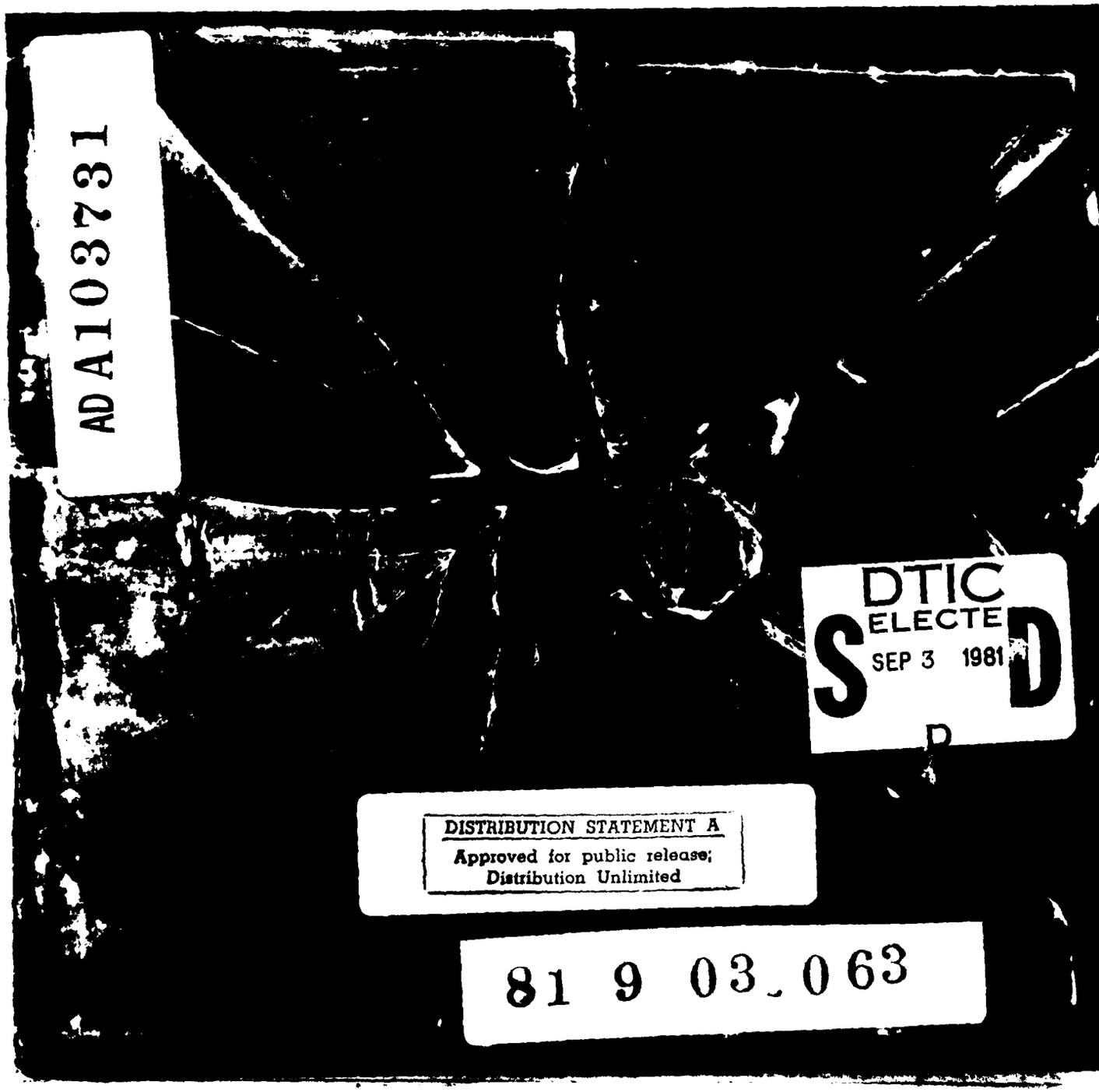

For conversion of SI metric units to U.S./British customary units of measurement consult ASTM Standard E380, Metric Practice Guide, *published by the American Society for Testing and Materials, 1916 Race St., Philadelphia, Pa. 19103.*

Cover: *Fractured ice plate. (Photograph by R. Demars.)*

CRREL Report 81-6

Investigation of the acoustic emission and deformation response of finite ice plates

P.C. Xirouchakis, M. Chaplin and W.F. St. Lawrence

April 1981

Prepared for
DIRECTORATE OF MILITARY PROGRAMS
OFFICE OF THE CHIEF OF ENGINEERS
By
UNITED STATES ARMY CORPS OF ENGINEERS
COLD REGIONS RESEARCH AND ENGINEERING LABORATORY
HANOVER, NEW HAMPSHIRE, U.S.A.

Unclassified

SECURITY CLASSIFICATION OF THIS PAGE (When Data Entered)

REPORT DOCUMENTATION PAGE	READ INSTRUCTIONS BEFORE COMPLETING FORM
1. REPORT NUMBER: CRREL ~~Report~~ 81-6	2. GOVT ACCESSION NO.: AD-A103 731
3. RECIPIENT'S CATALOG NUMBER	
4. TITLE (and Subtitle): INVESTIGATION OF THE ACOUSTIC EMISSION AND DEFORMATION RESPONSE OF FINITE ICE PLATES	5. TYPE OF REPORT & PERIOD COVERED
	6. PERFORMING ORG. REPORT NUMBER
7. AUTHOR(s): P.C. Xirouchakis, M. Chaplin and W.F. St. Lawrence	8. CONTRACT OR GRANT NUMBER(s)
9. PERFORMING ORGANIZATION NAME AND ADDRESS: Massachusetts ~~Institute of Technology~~, Cambridge, Massachusetts 02139; U.S. Army Cold Regions Research and Engineering Laboratory, Hanover, New Hampshire 03755	10. PROGRAM ELEMENT, PROJECT, TASK AREA & WORK UNIT NUMBERS: DA Project 4A161102AT24, ~~Task~~ B, Work Unit 003
11. CONTROLLING OFFICE NAME AND ADDRESS: Directorate of Military Programs, Office of the Chief of Engineers, Washington, D.C. 20314	12. REPORT DATE: April 1981
	13. NUMBER OF PAGES: 23
14. MONITORING AGENCY NAME & ADDRESS (if different from Controlling Office)	15. SECURITY CLASS. (of this report): Unclassified
	15a. DECLASSIFICATION/DOWNGRADING SCHEDULE

16. DISTRIBUTION STATEMENT (of this Report)

Approved for public release; distribution unlimited.

17. DISTRIBUTION STATEMENT (of the abstract entered in Block 20, if different from Report)

18. SUPPLEMENTARY NOTES

19. KEY WORDS (Continue on reverse side if necessary and identify by block number)

Acoustic emissions
Fracture (mechanics)
Ice
Plates

20. ABSTRACT (Continue on reverse side if necessary and identify by block number)

A procedure is described for monitoring the microfracturing activity in ice plates subjected to constant loads. Sample time records of freshwater ice plate deflections as well as corresponding total acoustic emission activities are presented. The linear elastic, as well as viscoelastic, response for a simply supported rectangular ice plate is given. Suggested future work using the above procedure is discussed.

DD FORM 1 JAN 73 1473 EDITION OF 1 NOV 65 IS OBSOLETE

Unclassified

SECURITY CLASSIFICATION OF THIS PAGE (When Data Entered)

037100

PREFACE

This report was prepared by P.C. Xirouchakis and M. Chaplin of the Department of Ocean Engineering, Massachusetts Institute of Technology, and by Dr. W.F. St. Lawrence, Geophysicist, of the Snow and Ice Branch, Research Division, U.S. Army Cold Regions Research and Engineering Laboratory.

Funding for this research was provided by DA Project 4A161102AT24, *Research in Snow, Ice and Frozen Ground*, Task B, *Cold Regions Environmental Interactions*, Work Unit 003, *Cold Regions Geophysical Processes*.

The authors wish to express their appreciation to the CRREL administration, and particularly to Dr. Andrew Assur, for providing the use of the necessary experimental facilities and instrumentation. Many thanks are given to Dr. W. Weeks for his encouragement of this work, and to Drs. D. Sodhi and K. O'Neill for technical review of the report.

CONTENTS

ILLUSTRATIONS

Figure

TABLES

Table

NOTATION

a, b	ice plate dimensions (Fig. A1)
c, d	loaded area dimensions (Fig. A1)
C	ice plate deflection coefficient (eq C2b)
D	ice plate flexural rigidity (eq A2)
E	Young's modulus
h	ice plate thickness
k_x, k_y, k_{xy}	ice plate middle surface change of curvatures (eq A7)
m, n	ice plate deflection mode numbers in the x and y directions respectively (eq A4)
M_x, M_y, M_{xy}	ice plate bending moments per unit length (Fig. A1)
p	ice load per unit loaded area
p_1, q_1	Maxwell model parameters (Fig. 6)
s	independent variable in the Laplace transform plane
t	time
U	ice plate bending strain energy (eq A1)
W	change in potential energy of applied load (eq A3)
x, y	ice plate Cartesian coordinates (Fig. A1)
z	coordinate normal to middle ice plate surface (Fig. A1)
ϵ	strain
η	ice plate transverse deflection
η_{mn}	ice plate transverse (ii) deflection component (eq A4)
μ	Poisson's ratio

INVESTIGATION OF THE ACOUSTIC EMISSION AND DEFORMATION RESPONSE OF FINITE ICE PLATES

P.C. Xirouchakis, M. Chaplin and W.F. St. Lawrence

INTRODUCTION

This report is the result of a preliminary investigation undertaken to examine the mechanical properties of ice undergoing flexural deformations. The primary purpose of this work was to study the time-dependent deformation of small simply supported ice plates and the microfracture properties as indicated by acoustic emission activity. Since the experiments conducted generally led to catastrophic failure of the ice plates, we were able to obtain information both on the loads that caused the plates to fracture and on the time to failure of the ice plate. Although this work represents a preliminary effort, we feel it is of some benefit in terms of establishing a method of testing finite ice plates. It also gives us some indication of magnitude of the loads which induce significant time-dependent deformation, microfracture and catastrophic failure of the ice.

A major problem encountered in our work was related to the development of a methodology for testing small ice plates subjected to loads that induced flexural deformation. Although a significant amount of work has been carried out on columnar-grained ice subjected to uniaxial compressive loads (for example, see Gold 1973 and Sinha 1978) we were unable to find work in the literature which related to flexural loading of small ice plates. Frederking and Gold (1974) did work on edge loaded ice plates and the report of their methodology was helpful in conducting this work.

Throughout the course of our three-week investigation we continually updated our experimental technique. We now feel that a viable method for examining the flexural response of simply supported ice plates has been established. Since our specimen size was small (plate surface area on the order of $1 m^2$) we were not able to load the ice plates while they were floating in the water in which they grew. Eventually we developed a support system that allowed us to measure considerable deflections of the ice plates while also allowing us to assume the plate to be simply supported.

The elastic solution for the deformation of a simply supported ice plate with the configuration of the ones tested is presented in Appendix A of this report. By applying the correspondence principle of linear viscoelasticity to the elastic solution for the plate deformation, we have also obtained the time-dependent viscoelastic solution for the deformation of a simply supported plate corresponding to our test configuration. In conjunction with this later solution we have measured the viscoelastic parameters, assuming the ice to be a Maxwell fluid.

A primary reason for conducting these experiments was to examine the acoustic emissions from ice subjected to flexural loads. The microfracture properties of ice in uniaxial compression have been examined by Gold (1972). However, no work has been reported which describes the microfracture of ice in flexure. To this end we monitored the ice plates using high-frequency (100- to 300-kHz) acoustic emission monitoring equipment. The results of this monitoring showed that the ice plate does emit stress waves that can be detected as acoustic emissions. However, at this juncture the results are far from being definitive. We do feel that this is a reasonable line of research to pursue.

In the course of our experiments we loaded all the

plates tested until they failed catastrophically. In several of the tests the fracture took place immediately upon application of the load. In several other tests significant time-dependent deformation took place before fracture was observed. From this we have obtained some information on the loads required to fracture a simply supported ice plate.

As a means of considering the structure of the ice, we made thin sections of all the ice plates tested after failure took place. This analysis allows us to consider our load deformation response and also the acoustic emission and fracture response in light of the grain structure of the material. We hope to use these data on crystal structures in the future not only to correlate structure with imposed parameters but also in controlling the nature of the ice structure being tested. In this series of experiments no attempt was made to influence the crystal growth; thus the ice tested grew under the influence of the variations in the coldroom environment and as a result the crystal structure varied significantly.

It was our plan to analyze and compare the behavior of freshwater ice, sodium chloride ice and urea ice. However, we found that given the time constraint imposed on our experiments (3 weeks) this was not possible to accomplish. In the future we hope to be able to complete this task. The purpose of this report, which is somewhat altered in terms of our original goals, is 1) to document our experimental effort, 2) to establish the analytic basis for examining plate deformation, and 3) to obtain preliminary information on the acoustic emission and failure properties of ice subjected to flexural loads. We hope that this report will be of some value to those who will continue to work along these lines.

EXPERIMENTAL PROCEDURE AND CONSIDERATIONS

A significant portion of the time allotted for this research endeavor was consumed in developing our experimental methodology. The instrumentation for measuring the deformation and acoustic emissions of the loaded ice plate followed standard procedures. The manner in which the ice plate was grown and the plate support system used required a significant number of trial and error attempts before we were satisfied that we were obtaining the desired test configuration. In this section we give a detailed description of the procedures used in growing and testing our ice plates, and also we describe the acoustic emission and load deformation system.

Growth of the ice plate

It was our goal to use relatively thin ice plates grown in a stress-free state. To facilitate this goal, a square plywood box with internal dimensions of 1.02 × 1.02 m and 0.6 m deep was used. The inside of the box was coated with an epoxy resin to make it watertight. Around the outside perimeter of the box, at approximately 0.45 m from the bottom, a heat tape was secured to the box. The heat tape was in turn connected to a voltage control device so that the heat generated could be regulated. The box, which was inside a coldroom, was then filled with distilled water to a depth of about 0.45 m, so that the water surface was at the same level as the heat tape. The coldroom for these tests was kept at a nominal temperature of -10°C.

By trial and error, a power setting was found for the heat tape at which the water at the edge of the box would not freeze while all other surface water would. To ensure that only the surface water of the box would freeze, the exterior sides of the box were insulated with 6 in. of foil-backed fiberglass insulation with a thermal resistance value rated at R 19. We found that a thin sheet of ice would form on the surface of the water when the temperature reached approximately -6°C just above the water surface in the -10°C coldroom. After a period of some 24 to 36 hours the thickness of the ice plate would be between 1 and 3 cm thick, at which point we considered the plate ready for testing. The ice plate temperatures were -10°C at the time of each test.

In all the tests conducted here we used distilled water as our fluid and did not make any attempt to seed the water surface to obtain a uniform grain size in our plates. However, it is possible that nucleation of the ice crystals making up the ice plate occurred during the defrost cycle of the coldroom, when a considerable number of nucleation particles are available in the air to seed the ice plate. To establish more control over our crystal structure in the future, we will use the powder snow seeding technique described by Frederking and Gold (1974).

Throughout the growth period of the plate, both the water and air temperature were monitored with copper-constantan thermocouples. When the plate was fully formed, a thermocouple was also frozen into the ice.

The ice plate of the size grown was larger than the plate we desired to test. To cut the plate to the proper dimensions immersion heaters (head bolt heaters for automobiles) were used. The temperature of the heaters was controlled with a voltage control device (Variac) to limit the heat ouput. If we failed to limit the power output of the heaters used for ice cutting, the heating element would invariably burn out. During the cutting

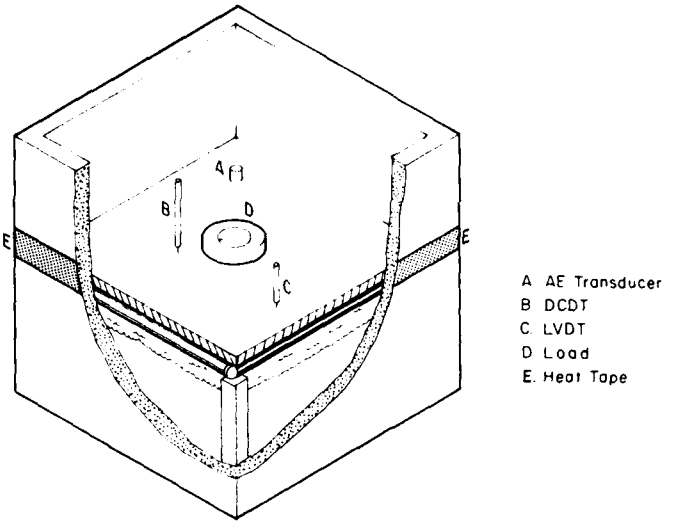

Figure 1. Ice plate support structure with a plate positioned on the structure. The area of load application is indicated.

process we noticed no indication of local ice fracture near the cutting instrument.

Support of the ice plate

A considerable effort was made to obtain a simple support system on which the ice plate could be tested. After some trial and error we arrived at a design which worked. We feel it is reasonable to mention two of our unsuccessful attempts so that these practices can be avoided in the future.

Our first idea was to use the water as the support system for the ice plate. However, we found that the forces required to deform the plate were larger than anticipated, so that the ice plate would flood when the load was applied. A second disadvantage of testing the ice plate while in contact with the water was that a strong temperature gradient existed across the plate. In our case with the coldroom at -10°C and the water at the base of the plate at +4°C, a temperature gradient of 14°C existed across the 1- to 2-cm-thick ice plate. This temperature gradient complicated the characterization of the experiment.

The second method that we used with limited success allowed us to place the ice plate on a platform made up of four iron bars arranged in a square within the tank. These bars were placed into the tank 5 to 10 cm below the surface of the water. When freezing of the ice sheet was completed and the ice plate had been trimmed to size, water was siphoned from the tank until the water surface was some 5 to 10 cm below the top of the support bar. The ice plate came to rest on the support structure when the water was lowered below the level of the constraining bars. The chief drawback with this method was that, since the bottom of the plate and also the support bars were wet, the plate tended to freeze to them. This complicated the boundary condition of the plate since it produced a bending resistance at the plate edge.

The method that finally evolved and which proved very satisfactory was a variation of the method described above. After the plate was cut to size it was removed from the tank. The water was then lowered and the plate was placed on the supporting structure for testing after the support bars and underside of the ice were dry. This kept the plate from freezing to the bars and bending resistance at the boundary was eliminated.

For future work we feel that the support structure could be totally removed from the freezing tank. In this manner the number of tests could be increased because a second plate could be growing while the first plate was tested. This would increase the number of plates that could be tested in a given time interval.

An illustration of the support structure for the ice plate with a plate in position and the load applied is shown in Figure 1. The bars that support the plate are 32 mm in diameter and 0.85 m long. The plate is supported on its perimeter by the bars on a square that is 0.77 m on each side. A plan view of the support structure including the transducer location is shown in Figure 2.

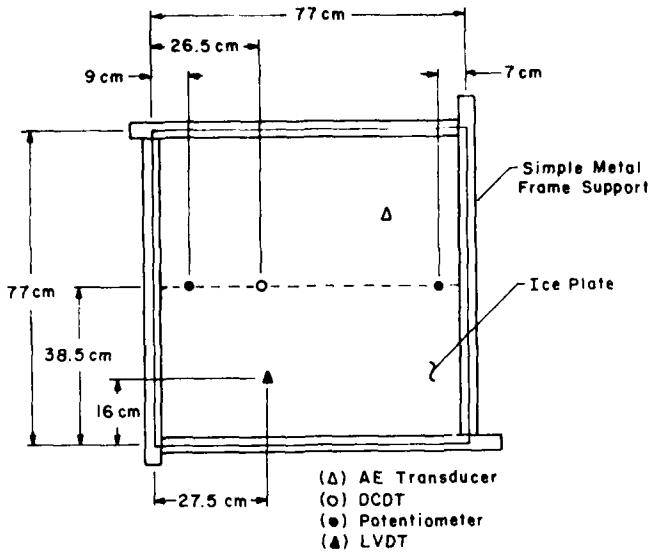

Figure 2. Plan view of the support structure and ice plate showing the position of the transducers.

To facilitate the recovery of the transducers and the loading weights after the ice failed, a plywood platform was placed beneath the ice plate. This platform allowed recovery of the fractured pieces of ice for examination at the completion of the test.

Acoustic emission monitoring system

We monitored the acoustic emissions from the ice as it deformed with an Acoustic Emission Technology Corporation Model 204B monitoring system. This system is typical of acoustic emission systems used for monitoring stress waves generated from various sources in materials. For these tests the data were processed in terms of the total number of acoustic events detected over the duration of the test.

We assume that the source of the acoustic emissions in our ice is the formation of small cracks and microcracks. This interpretation is consistent with the correlation between acoustic emissions and small fractures in ice observed by Gold (1960). In our experiments the threshold at which acoustic emissions are detected is well below the limit of visible fractures in ice.

Figure 3 is a plot of the calibration curve for the transducer as a function of frequency in MHz. For the amplifiers used in these experiments the bandpass between -3-dB points was 100 to 300 kHz. The transducer calibration curve (Fig. 3) suggests that we would detect the acoustic emissions at the resonance peak with a sensitivity of -70 dB (re 1 V/μbar) at just over 150 kHz. For our test the amplifier was set to a gain of 84 dB and the threshold detection level set between 0.059 V and 1.43 V. These system parameters indicate that, for a signal to be detected, the signal at the transducer had to have a minimum intensity of 0.0013 Pa for the 0.59-V threshold setting and an intensity of 0.0285 Pa at the detector for the 1.43-V threshold setting. (See Appendix B for details on these determinations.)

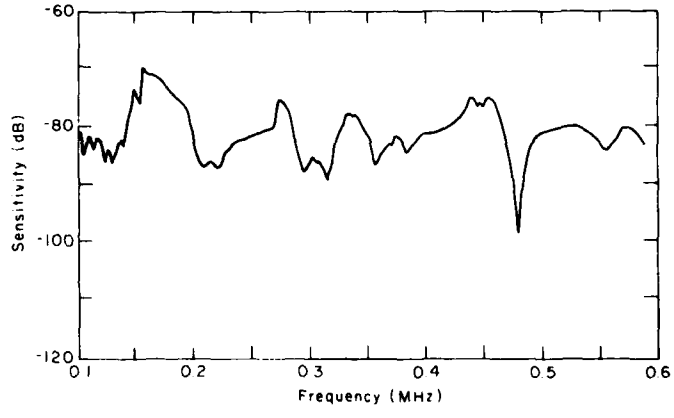

Figure 3. Acoustic emission transducer calibration curve.

Two methods were used to couple the acoustic emission transducers to the ice plate. For the first test the transducer was frozen directly to the ice plate in the position indicated in Figure 3. For succeeding tests the transducer was interfaced with the ice surface using a silicone high vacuum grease.

To test the system response, a 0.5-mm pencil lead was broken on the plate at a position diagonally opposite the acoustic emission transducer. This demonstrated that a signal of this amplitude could be detected at a distance of approximately 0.75 m from the transducer. For our experiment we assumed that most of the signals detected at the 84-dB gain level occurred in the ice plate.

Displacement transducers and data recording

A number of different displacement transducers were used in this experiment, as indicated in Figure 2. The load was applied at the center of the ice plate and a direct current deformation transducer (DCDT) was mounted at the center line of the plate 12 cm from the central point of the plate. A linear variable differential transducer (LVDT) was also used to measure the plate deflection at a point 11 cm to the left of the plate center and 22 cm below the DCDT as viewed in Figure 2. As indicated in this figure, we attempted to use two linear potentiometers but found that these did not have the sensitivity to measure the deflections observed.

The transducers and the acoustic emission preamplifier were supported on a beam that extended across the test tank. A photograph of the test system including the loading weights is shown in Figure 4. In this photograph we have labeled each test piece.

The data from the DCDT and the acoustic emission system were recorded on a strip chart recorder. Data from the LVDT, the three thermocouples, the DCDT, and the acoustic emission monitoring system were recorded on a data logger. The interval between data acquisition periods varied depending on which phase a particular test was in.

Mechanical loading system

All tests were conducted in a constant load configuration. Weights were applied at the center of the ice plate as indicated in Figures 1 and 2. To eliminate noise generation between the load and the ice plate a cloth mat was used to isolate the load. This helped

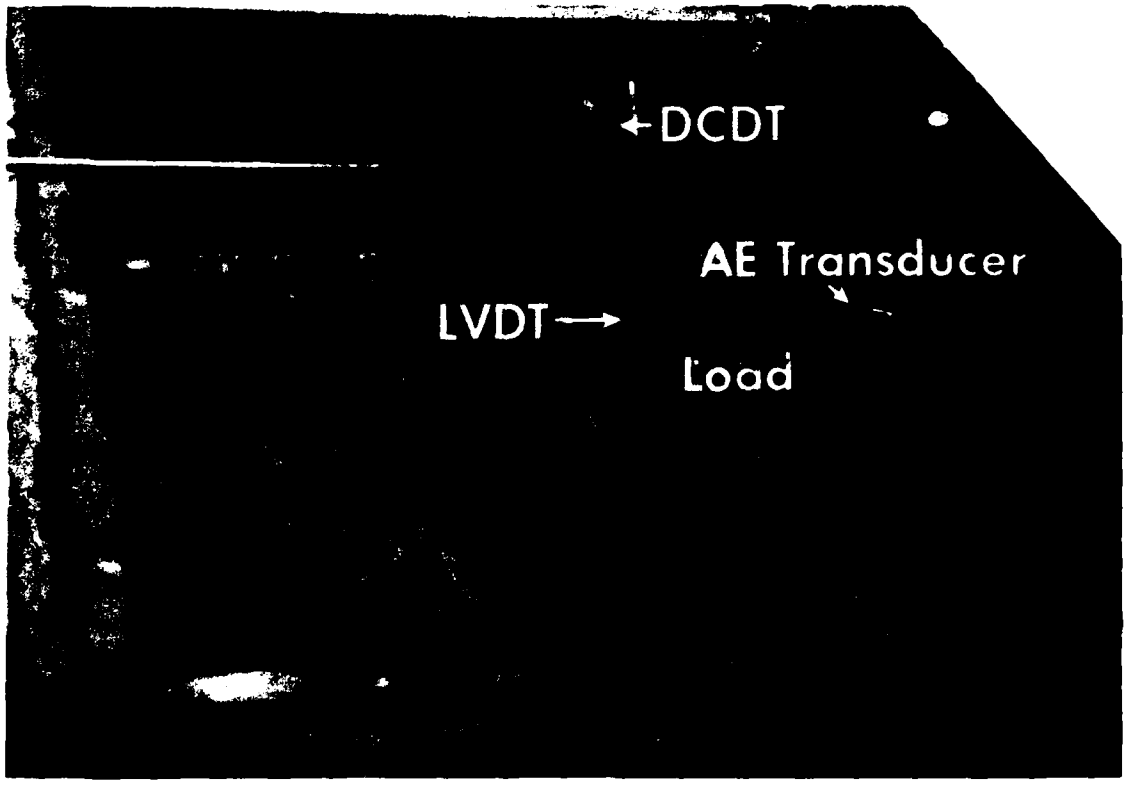

Figure 4. Photograph of the test setup with each piece of test equipment indicated.

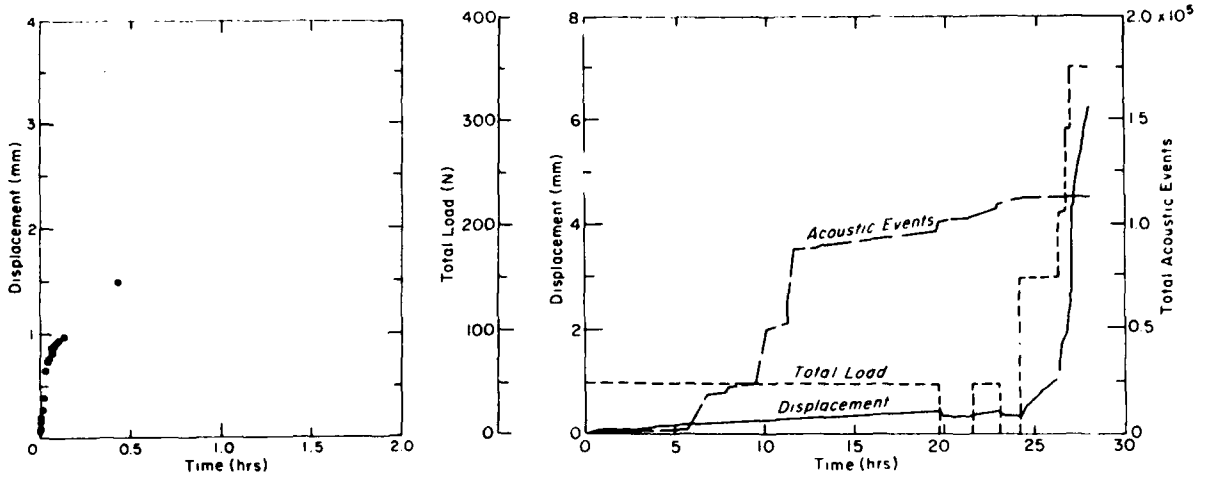

a. Test 1. *b. Test 2.*

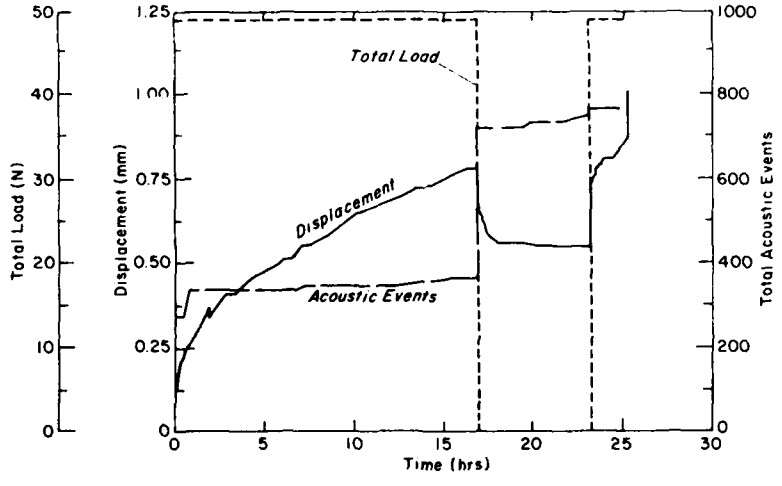

c. Test 4.

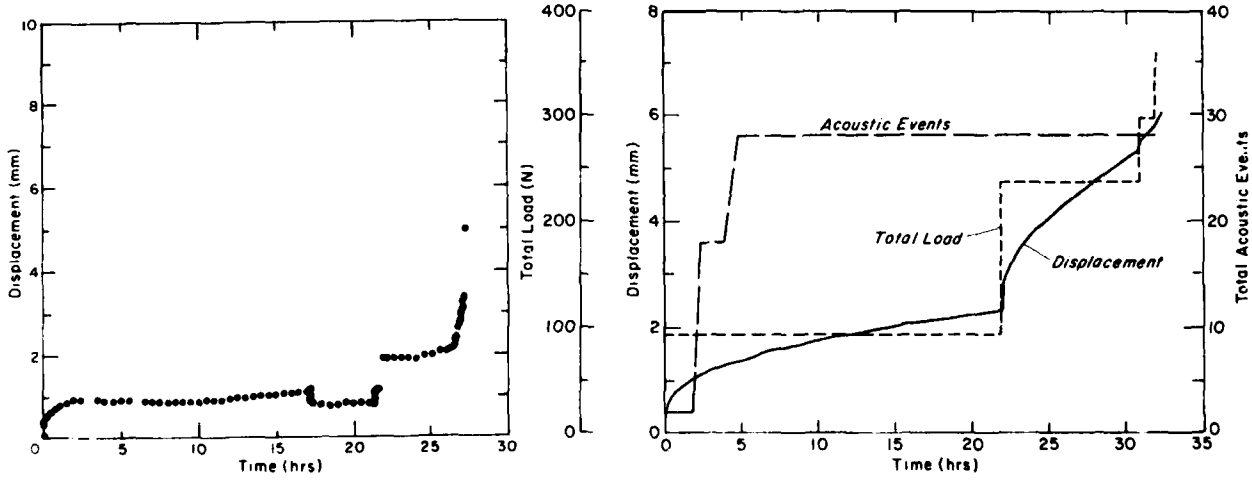

d. Test 5. *e. Test 7.*

Figure 5. Deformation and acoustic emission data from ice plate tests.

ensure that no extraneous acoustic emissions were generated.

ANALYSIS

Nevel (1966) has analyzed the time-dependent behavior of an ice plate of infinite extent. However, due to the dimensions of our experimental ice plate, it was necessary for us to seek a solution in terms of finite plate theory. It was also necessary, in view of our experimental arrangement, to consider the load to be distributed over a finite extent of the ice plate.

In Appendix A, the elastic solution for the deflection of a finite ice plate with a distributed load is developed. The solution is presented in terms of the deflection, curvatures and bending moments developed in the ice plate.

In order to examine the time-dependent deformation of the ice plate, we have solved for the viscoelastic response of the plate by applying the correspondence principle of linear viscoelasticity. The solutions for the viscoelastic deformation, curvatures and bending moments are developed in Appendix C. To obtain this solution we assume that the ice behaves as a Maxwell fluid. In Appendix C we also develop the solution when the weight of the plate is considered.

EXPERIMENTAL RESULTS

In this experiment six ice plates were tested. Each of the ice plates was grown as described in the section on experimental procedure. The ice plates generally took 24 to 36 hours to grow and were between 1 and 2 cm thick. The results varied considerably from test to test even though the growth history of each ice plate was similar.

The first ice plate that was tested had an average ice thickness of 1.9 cm. A load of 196 N was applied to the center of the plate, and the plate failed approximately 45 minutes after the load application. Unfortunately, few data points were recorded (Fig. 5a) so that the estimation of Maxwell's constants could not be reliably made. The second ice plate that was tested had an average ice thickness of 1.5 cm. After the plate was formed, a load of 49 N was applied to the center. The plate deformation was monitored at one point, near the center of the plate (see Fig. 2).

Figure 5b shows that the deformation rate of the second plate achieved a constant value after loading, and continued to deform at that rate until the 49-N load was removed some 20 hours after its application. The maximum deflection of the ice plate, as measured by the DCDT, was 0.46 mm in the 20-hour time interval.

The acoustic emission count from the initial loading phase of this test shows little organization. That is, we observed no regular pattern of acoustic activity for this loading. However, there were several periods of increased emissions – perhaps indicative of local yielding at points throughout the plate. For this test, the acoustic emission sensitivity was much higher than for the succeeding tests. It was set to detect signals above a threshold of 0.75 V or 0.015 Pa calculated in accordance with the procedure described in Appendix B.

When the load was removed, the ice plate was allowed to relax for a period of about two hours. The initial recovery of the ice plate occurred within one hour of unloading. Little or no recovery was observed after this time.

The ice plate was then loaded and unloaded through several cycles until the plate's eventual failure (Fig. 5b). Unlike the initial phase of this test, the acoustic emission count during the loading–unloading cycles showed a rather regular pattern, typically at a rate of 100 counts per minute. This may indicate that local, isolated yielding occurs only during the initial loading of an unstressed ice plate.

The third ice plate tested was subjected to a different load history than the first two plates. In this test we intended to apply a 250-N load in increments of about 40 N. The total load was to be applied within one minute. In this test the ice plate (with a mean thickness of 1.7 cm) failed when the load reached 157 N. Acoustic emissions were observed throughout the loading of the plate until the time it failed.

In the next test (Fig. 5c), the plate was again preloaded with a 49-N load. For this test the threshold intensity at which acoustic emissions were to be detected was increased from 0.015 Pa to 0.035 Pa, which was 2.3 times greater than in the previously described experiments.

During the application of the 49-N load, some 350 emissions were detected at this threshold level. The plate had a mean thickness of 0.9 cm.

The specimen was then unloaded, allowed to recover, and reloaded first to 49 N and then to 154 N. The ice plate failed when the 105-N increment was applied to bring the load to 154 N. Not many acoustic emissions were recorded during this test, due perhaps to the increased threshold level setting.

The last two tests (Fig. 5d, 5e) were conducted using nearly equal loads. The second of these tests (Fig. 5e) was initially loaded to 93 N and allowed to deform for a 22-hour period. The load was then increased to 236 N. The plate continued to deform for 11 hours under this load, until the test was terminated. The ice plate had a mean thickness of 1.5 cm. The acoustic emission data from this test are unreliable due to poor coupling between the transducer and the ice plate.

Table 1. Summary of tests conducted.

	Applied load P (N)	Plate thickness h (mm)	Maxwell's constants q_1/p_1 (N/m²)	p_1 (hr)	Avg. grain size (mm) (surface projection)
Test 1	196	19	*	*	
Test 2	49	15	25.522×10^{9}	1.128	5.8
Test 3	157	17	†	†	8
Test 4	49	9	9.286×10^{9}	11.268	10
Test 5	109	13	2.237×10^{9}	47.059	11.7
Test 6	93	15	0.904×10^{9}	28.261	6.7

* Printer failure on data acquisition system does not permit reliable material parameter estimation.
† Instantaneous failure.

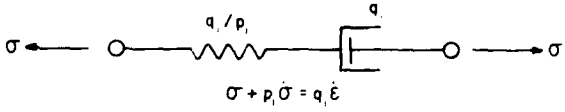

Figure 6. Elements of the Maxwell model with the parameters identified as specified in Table 1.

The reduction of the load deformation data when considering the initial phase of loading gave the values of the ice plate material parameters summarized in Table 1. The weight of the ice plate cannot be neglected in comparison to the applied load and therefore has been taken into account when determining the ice plate response (see Appendix C). The Maxwell rheological model (Fig. 6) material parameters q_1/p_1 (elastic modulus) and p_1 (viscous time constant) were determined and are reported in Table 1. Considerable scatter in the obtained values is probably due to the grain size and ice plate thickness variation. For instance, the ice plate of test 3, with about the same thickness as test 1 and a smaller applied load, failed instantaneously, whereas some 45 minutes elapsed before the plate of test 1 collapsed. We found that, upon adding a 143-N increment of load in test 6, the resulting tangent modulus increased from 9.04×10^{8} to 2.134×10^{5} N/m² and the viscous time constant decreased from 28.261 to 3.692 hours. This result indicates that in this instance subjecting the plate to a prior load (93 N) produced a more rigid ice plate.

THIN SECTION ANALYSIS

After each test was completed, samples of the ice were collected and placed in a cold storage area at a temperature of -30°C. When all the tests were completed, thin sections from each ice plate were prepared.

The thin section analysis indicated that there was a large variation in the grain size of the ice crystals in the ice plates. Generally, however, the ice crystals in a single ice plate were fairly consistent. Single crystals extended the full depth of each plate.

Figure 7 shows the characteristic grain structure of the ice plates tested. The average grain diameter is determined by counting the number of grains along a length of straight line in the thin section (Fig. 7b) and dividing that number into the length of line over which the grains are counted. The last column of Table 1 lists the mean grain diameters from each plate found using this technique. For the six tests conducted, the mean grain diameter varied by as much as a factor of two from the smallest grains to the largest grains.

The stress fringes visible in Figure 7 are the result of thermal stressing introduced during thin section preparation and are not associated with the deformation of the ice plate.

SUMMARY AND DISCUSSION

As previously indicated, this report represents an initial investigation into the flexural properties of ice. It was also intended to examine the feasibility of using acoustic emission techniques for these investigations. Considering the limited time in which the work was carried out, we feel that the investigation was successful in meeting these objectives.

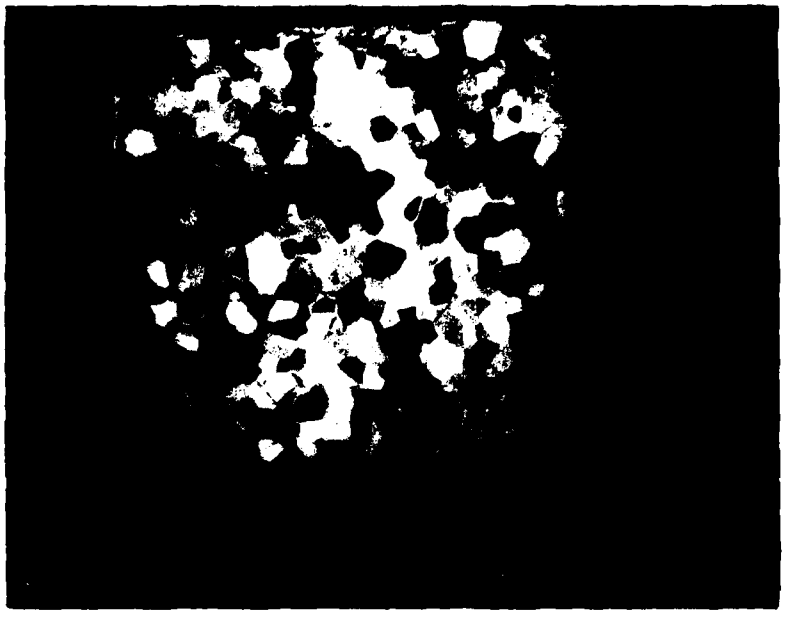

a. Surface parallel thin section.

b. Surface perpendicular thin section.

Figure 7. Thin section from the ice plate from test 1 made after failure of the ice plate.

One of the most interesting phenomena we observed in these tests had to do with the failure of the ice plates. In the cases in which the ice plate failed at some time after application of the load, we could not detect any accelerating creep that might indicate an impending failure. Similarly, although we generally detected acoustic emissions associated with loads that produced failure, we did not see any acceleration of the emission rate. This finding appears to indicate that it may be difficult to predict an impending failure in flexure. However, it may be that failure will always follow when the deformation rate exceeds

some value or when acoustic emissions are detected. These points should be investigated in future work.

LITERATURE CITED

Flugge, W. (1975) *Viscoelasticity*. New York: Springer-Verlag.

Frederking, R. and L. Gold (1974) Model study of edge loading of ice covers. *Proceedings 27th Canadian Geotechnical Conference*. Edmonton, Alberta.

Gold, L. (1960) The cracking activity in ice during creep. *Canadian Journal of Physics*, vol. 38, p. 1137-1148.

Gold, L. (1972) The process of failure of columnar-grained ice. *Philosophical Magazine*, vol. 26, p. 311-328.

Gold, L. (1973) Activation energy for creep of columnar-grained ice. In *Physics and Chemistry of Ice* (E. Whalley, S.J. Jones and L.W. Gold, Eds.). Ottawa: Royal Society of Canada, p. 362-364.

Nevel, D.E. (1966) Time-dependent deflection of a floating ice sheet. CRREL Research Report 196. AD 638717.

St. Lawrence, W. (1979) A phenomenological description of the acoustic emission response in several polycrystalline materials. *Journal of Testing and Evaluation*, vol. 7, p. 223-228.

Sechler, E.E. (1952) *Elasticity in Engineering*. New York: John Wiley and Sons.

Sinha, N.K. (1978) Rheology of columnar-grained ice. *Experimental Mechanics*, vol. 18, no. 12, p. 464-470.

APPENDIX A: ICE PLATE LINEAR ELASTIC RESPONSE

The linear elastic response of a simply supported rectangular plate subjected to uniformly distributed loading (perpendicular to the plane of the plate) over part of the plate surface (Fig. A1) is developed. Small displacement theory is assumed. The Rayleigh-Ritz procedure is utilized.

The bending strain energy U stored in the plate during deformation (Sechler 1952) is

$$U = \frac{1}{2} D \int_0^a \int_0^b \left\{ \left(\frac{\partial^2 \eta}{\partial x^2} + \frac{\partial^2 \eta}{\partial y^2} \right)^2 - 2(1-\mu) \left[\frac{\partial^2 \eta}{\partial x^2} \frac{\partial^2 \eta}{\partial y^2} - \left(\frac{\partial^2 \eta}{\partial x \partial y} \right)^2 \right] \right\} dx dy \tag{A1}$$

where η = the plate deflection

μ = Poisson's ratio

D = the plate flexural rigidity $[Eh^3/12(1-\mu^2)]$ (A2)

h = plate thickness

E = Young's modulus.

The change in potential energy W of the applied load per unit area p is

$$W = p \int_{\frac{a-c}{2}}^{\frac{a+c}{2}} \int_{\frac{b-d}{2}}^{\frac{b+d}{2}} \eta \, dx dy. \tag{A3}$$

Since simple support conditions prevail on all four edges of the plate, the deflection is expanded in the following series:

$$\eta = \sum_m^\infty \sum_n^\infty \eta_{mn} \sin \frac{m\pi x}{a} \sin \frac{n\pi y}{b} . \tag{A4}$$

The bending strain energy and change in potential energy of the applied load expression are reduced to

$$U = \frac{\pi^4 ab}{8} D \sum_m^\infty \sum_n^\infty \eta_{mn}^2 \left(\frac{m^2}{a^2} + \frac{n^2}{b^2} \right)^2 \tag{A5a}$$

and

$$W = 4p \frac{ab}{\pi^2} \sum_m^\infty \sum_n^\infty \eta_{mn} \frac{1}{mn} \sin \frac{m\pi}{2} \sin \frac{n\pi}{2} \sin \frac{m\pi c}{2a} \sin \frac{n\pi d}{2b} . \tag{A5b}$$

Minimizing the total energy in the system U-W with respect to the amplitude term η_{mn} yields:

$$\eta_{mn} = \frac{16p}{\pi^6 D} \frac{\sin \frac{m\pi c}{2a} \sin \frac{n\pi d}{2b}}{mn \left(\frac{m^2}{a^2} + \frac{n^2}{b^2} \right)^2} \tag{A6}$$

where m and n are odd. The middle surface curvature changes k_x, k_y, k_{xy} are given by

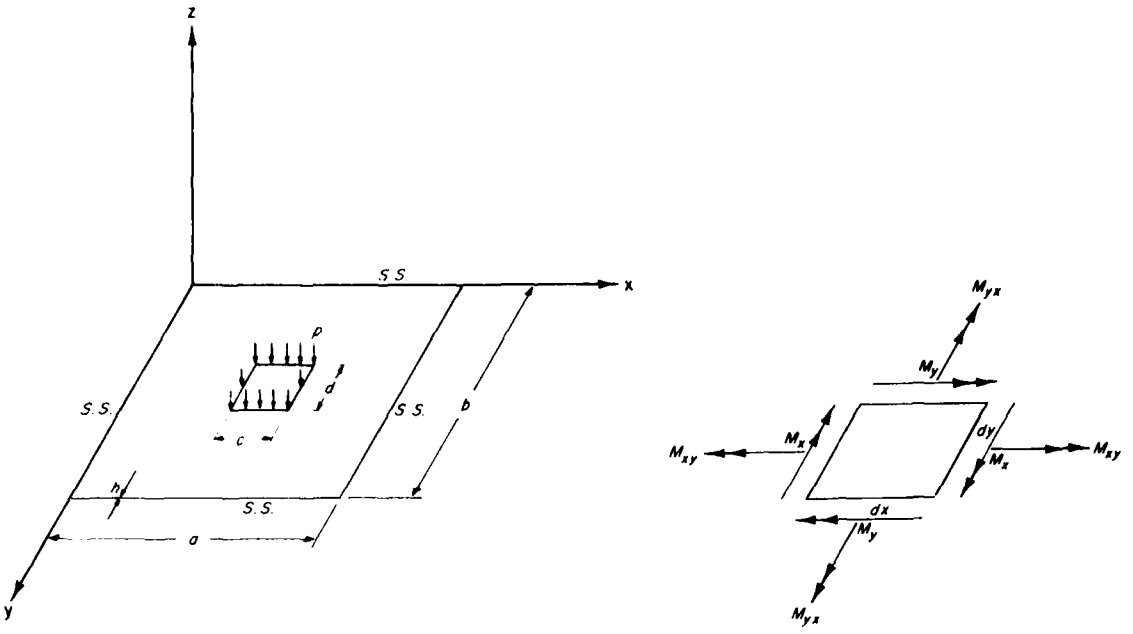

Figure A1. Rectangular plate subjected to distributed loading.

$$k_x = \frac{\partial^2 \eta}{\partial x^2} = \sum_m^\infty \sum_n^\infty -\left(\frac{m\pi}{a}\right)^2 \eta_{mn} \sin\frac{m\pi x}{a} \sin\frac{n\pi y}{b} \tag{A7a}$$

$$k_y = \frac{\partial^2 \eta}{\partial y^2} = \sum_m^\infty \sum_n^\infty -\left(\frac{n\pi}{b}\right)^2 \eta_{mn} \sin\frac{m\pi x}{a} \sin\frac{n\pi y}{b} \tag{A7b}$$

$$k_{xy} = \frac{\partial^2 \eta}{\partial x \partial y} = \sum_m^\infty \sum_n^\infty \left(\frac{mn\pi^2}{ab}\right) \eta_{mn} \cos\frac{m\pi x}{a} \cos\frac{n\pi y}{b} . \tag{A7c}$$

The bending moments M_x, M_y, M_{xy} are given by

$$M_x = D\left(\frac{\partial^2 \eta}{\partial x^2} + \mu \frac{\partial^2 \eta}{\partial y^2}\right) = \sum_m^\infty \sum_n^\infty -\pi^2 D\left(\frac{m^2}{a^2} + \mu \frac{n^2}{b^2}\right) \eta_{mn} \sin\frac{m\pi x}{a} \sin\frac{n\pi y}{b} \tag{A8a}$$

$$M_y = D\left(\frac{\partial^2 \eta}{\partial y^2} + \mu \frac{\partial^2 \eta}{\partial x^2}\right) = \sum_m^\infty \sum_n^\infty -\pi^2 D\left(\frac{n^2}{b^2} + \mu \frac{m^2}{a^2}\right) \eta_{mn} \sin\frac{m\pi x}{a} \sin\frac{n\pi y}{b} \tag{A8b}$$

$$M_{xy} = D(1-\mu) \frac{\partial^2 \eta}{\partial x \partial y} = \sum_m^\infty \sum_n^\infty \pi^2 D(1-\mu) \frac{mn}{ab} \eta_{mn} \cos\frac{m\pi x}{a} \cos\frac{n\pi y}{b} . \tag{A8c}$$

Equation A6 for the deflection amplitude term η_{mn} and eq A4, A7 and A8 for determining the deflection, curvature changes and bending moments constitute the elastic solution for the deflection of a finite plate subjected to a distributed load.

APPENDIX B: ACOUSTIC EMISSION SYSTEM SENSITIVITY

The sensitivity of acoustic emission systems is often given in terms of the gain of the amplification system used to monitor the acoustic emissions. This gain figure (in decibels) is generally accepted by acoustic emission workers in terms of an implied assumption that the band width of the acoustic emission (AE) system and the transducer sensitivity are within familiar limits. However, to be somewhat more specific we can relate the AE sensitivity to either the signal voltage at the preamplifier input or to the stress wave intensity at the transducers.

In the text we state that we used a system gain of 84 dB and our threshold level was set between 0.059 and 1.43 V. These threshold settings indicate that for a signal to be recognized as an acoustic event, its amplitude, when amplified, must exceed these threshold voltage settings.

The numerical gain associated with 84 dB can be determined from the formula

$$G = 10^{dB/20}. \tag{B1}$$

For 84 dB, the numerical gain is $G = 15{,}849$ which allows us to calculate the signal amplitude from the transducer to be between

$$\frac{0.059\ \text{V}}{15{,}849} = 3.723\times 10^{-6}\ \text{V}$$

and

$$\frac{1.43\ \text{V}}{15{,}849} = 9.023\times 10^{-5}\ \text{V}$$

or approximately between 4 and 90 μV. According to the manufacturer's calibration data, the peak sensitivity of the transducer used is -70 dB (re 1 V/μbar) at a frequency slightly larger than 150 kHz (see Fig. 3). If we assume that our signal amplitude corresponds to the peak transducer sensitivity, we can calculate a nominal amplitude of the stress wave at the transducer.

Using the formula for amplitude gain

$$E_0 = E_r\, 10^{0.05\ \text{dB}} \tag{B2}$$

where E_0 = output voltage per unit stress
E_r = reference value (i.e. 1 V/μbar or 10 V/Pa)
dB = transducer sensitivity (i.e. -70 dB).

Then substituting the given values in eq B2, we find the calibration value E_0 to be

$$E_0 = \left(\frac{1\ \text{V}}{\mu\text{bar}}\right) 10^{0.05(-70)} = 3.162\times 10^{-4}\ \frac{\text{V}}{\mu\text{bar}} \tag{B3}$$

or equivalently

$$E_0 = 3.162\times 10^{-3}\ \frac{\text{V}}{\text{Pa}}$$

since 1 μbar = 0.1 Pa.

So if the threshold sensitivity is set such that the transducer output voltage of 4 μV or 90 μV is required to register an event, the corresponding stress intensity thresholds are between

$$\frac{4\times10^{-6}\ \text{V}}{3.162\times10^{-3}\ \text{V/Pa}} = 1.265\times10^{-3}\ \text{Pa}$$

and

$$\frac{90\times10^{-6}\ \text{V}}{3.162\times10^{-3}\ \text{V/Pa}} = 28.46\times10^{-3}\ \text{Pa}$$

which are the values reported in the text.

Although all acoustic emission equipment manufacturers now calibrate their transducers by referencing them to the 1 V/μbar setting there are no data to suggest that this value is either absolute or correct. Indeed one manufacturer (Dunegan/Endevco) suggests that the current calibration method which relates output voltage to stress is not valid at all. Dunegan/Endevco suggests that the proper calibration should be in terms of velocity [i.e. dB re 1V/(m/s)]. The stress figures are calculated above so that we can have a basis of comparison.

APPENDIX C: ICE PLATE LINEAR VISCOELASTIC RESPONSE

The assumption is made that ice is incompressible under hydrostatic stress and obeys Maxwell's model (Fig. 6) for deviatoric stress and strain (Nevel 1966). The viscoelastic response can be obtained from the corresponding elastic one using the correspondence principle (Flügge 1975). Thus making the following substitutions

$$E \rightarrow \frac{3q_1 s}{2(1+p_1 s)} \tag{C1a}$$

$$\mu \rightarrow \tfrac{1}{2} \tag{C1b}$$

into equation A6, the Laplace transform of the amplitude term $\bar{\eta}_{mn}$ is

$$\eta_{mn} = C\frac{1+p_1 s}{s^2} \tag{C2a}$$

where m and n are odd and

$$C = \frac{96p}{\pi^6 q_1 h^3}\,\frac{\sin\frac{m\pi c}{2a}\sin\frac{n\pi d}{2b}}{mn\left(\frac{m^2}{a^2}+\frac{n^2}{b^2}\right)^2} \tag{C2b}$$

and a step function loading

$$p(t) = p\Delta(t) \tag{C2c}$$

has been assumed. Taking the inverse Laplace transform, the deflection amplitude term η_{mn} is given by

$$\eta_{mn} = C[t+p_1\Delta(t)]. \tag{C3}$$

Equation A4 together with eq C3 provides the plate deflection for the assumed viscoelastic material.

The middle surface curvature changes k_x, k_y, k_{xy} can be obtained from eq A7 provided that eq C3 is used for η_{mn}. Finally the bending moments M_x, M_y, M_{xy} are given by

$$M_x = \sum_m^\infty \sum_n^\infty -\pi^2\frac{h^3}{6}q_1 C\left(\frac{m^2}{a^2}+\frac{1}{2}\frac{n^2}{b^2}\right)\Delta(t)\sin\frac{m\pi x}{a}\sin\frac{n\pi y}{b} \tag{C4a}$$

$$M_y = \sum_m^\infty \sum_n^\infty -\pi^2\frac{h^3}{6}q_1 C\left(\frac{n^2}{b^2}+\frac{1}{2}\frac{m^2}{a^2}\right)\Delta(t)\sin\frac{m\pi x}{a}\sin\frac{n\pi y}{b} \tag{C4b}$$

$$M_{xy} = \sum_m^\infty \sum_n^\infty -\pi^2\frac{h^3}{12}q_1 C\frac{mn}{ab}\Delta(t)\cos\frac{m\pi x}{a}\cos\frac{n\pi y}{b}. \tag{C4c}$$

Solution considering the weight of the ice plate

For simplicity assume $a = b$ and $c = d$. Then eq C2b reduces to

$$C = \frac{96}{\pi^6} \frac{pa^4}{q_1 h^3} \frac{\sin \frac{m\pi c}{2a} \sin \frac{n\pi c}{2a}}{mn(m^2+n^2)^2} \tag{C5}$$

Deflections η_{mn} due to the load of magnitude p extended over the area c by d are given by eq C3 with C from eq C5. Deflections η_{mn} due to ice plate weight of magnitude p_1 extended over the area a by b are given by eq C3 with C_{IW} from eq C6:

$$C_{\substack{IW \\ m,n\ odd}} = \frac{96}{\pi^6} \frac{p_1 a^4}{q_1 h^3} \frac{1}{mn(m^2+n^2)^2} . \tag{C6}$$

Keeping only the first term in the series $m = n = 1$, from eq C5

$$C = \frac{24}{\pi^6} \frac{pa^4}{q_1 h^3} \sin^2 \frac{\pi c}{2a}$$

from eq C6

$$C_{IW} = \frac{24}{\pi^6} \frac{p_1 a^4}{q_1 h^3}$$

or

$$\frac{C_{IW}}{C} = \frac{1}{\sin^2 \frac{\pi c}{2a}} \frac{p_1}{p} \tag{C7}$$

i.e.

$$\eta_{11} = C \left(1 + \frac{1}{\sin^2 \frac{\pi c}{2a}} \frac{p_1}{p}\right) \left[t + p_1 \Delta(t)\right]$$

to take into account the weight of the ice plate multiply C by $1 + C_{IW}/C$.

Solution considering an increment in applied pressure

Δp at time $t_{\Delta p}$

Equation C2c now becomes

$$p(t) = p\Delta(t) + (\Delta p)\, \Delta(t - t_{\Delta p}) \tag{C8}$$

and its Laplace transform is

$$\bar{p} = \frac{p}{s} \left[1 + \frac{\Delta p}{p} e^{-t_{\Delta p} s}\right]$$

thus eq C3a now becomes

$$\overline{\eta_{mn}} = C\left(1 + \frac{\Delta p}{p}\, e^{-t_{\Delta p} s}\right)\frac{(1+p_1 s)}{s^2} \tag{C9}$$

and eq C3 now becomes

$$\eta_{mn} = C[t+p_1\,\Delta(t)]+C\frac{\Delta p}{p}\,[(t-t_{\Delta p})+p_1\Delta(t-t_{\Delta p})]. \tag{C10}$$

Solution considering an increment in applied pressure Δp at time $t_{\Delta p}$ plus the weight of the ice plate

Equation C2c now becomes

$$p(t) = (p+p_1)\,\Delta(t)+(\Delta p)\,\Delta(t-t_{\Delta p}); \tag{C11}$$

thus eq C2a now becomes for $m = n = 1$

$$\overline{\eta_{11}} = C(p)\left(1 + e^{-t_{\Delta p} s}\,\frac{\Delta p}{p} + \frac{p_1}{p}\,\frac{1}{\sin^2\frac{\pi c}{2a}}\right) \tag{C12a}$$

where

$$C(p) = \frac{24}{\pi^6}\,\frac{pa^4}{qh^3}\,\sin^2\frac{\pi c}{2a}\left(\frac{1+p_1 s}{s^2}\right). \tag{C12b}$$

Equation C3 now becomes

$$\eta_{11} = C\left\{\left[1 + \frac{p_1}{p}\,\frac{1}{\sin^2\frac{\pi c}{2a}}\right]\left[t+p_1\,\Delta(t)\right] + \frac{\Delta p}{p}\left[(t-t_{\Delta p})+p_1\Delta(t-t_{\Delta p})\right]\right\}. \tag{C13}$$

APPENDIX D: EQUIPMENT LIST

Instrument	*Manufacturer*	*Model*	*Quantity*
General equipment list			
Datalogger	Monitor Labs.	9300	1
Regulated power supply	Power Mate Co.		
Strip chart recorder	Soltec, Inc.	VP-67325	
Linear position differential transducer (potentiometer)	Bourns Instr.	PN2001091701	2
Linear voltage differential transformer (LVDT)	Schaevitz Eng.	TR-100R	
LVDT transducer readout	Schaevitz Eng.	TR 100R	
Direct current differential transducer (DCDT)	Sanbourn Man.	7DCDT-3000	1
Headbolt engine heaters	Freeman		2
Variable transformer	Sup. Elec. Co.	116	1
0.001-mm calibration instrument	Starret Co.		1
Thermocouples			4
Salinometer and pipettes*	Beckman	RB3,CEL-G20	1
Acoustic emission (AE) equipment list			
Battery charger	A.E. Tech. Corp.	204 Bat. Chg.	1
Preamp	A.E. Tech. Corp.	0204010	1
Amplifier	A.E. Tech. Corp.	0204023	1
A.E. transducer	A.E. Tech. Corp.	AC175L	1

* For saltwater ice plate experiments.

A facsimile catalog card in Library of Congress MARC format is reproduced below.

Xirouchakis, P.C.
Investigation of the acoustic emission and deformation response of finite ice plates / by P.C. Xirouchakis, M. Chaplin and W.F. St. Lawrence. Hanover, N.H.: U.S. Cold Regions Research and Engineering Laboratory; Springfield, Va.: available from National Technical Information Service, 1981.
iv, 23 p., illus.; 28 cm. (CRREL Report 81-6.)
Prepared for Directorate of Military Programs, Office of the Chief of Engineers by Corps of Engineers, U.S. Army Cold Regions Research and Engineering Laboratory under DA Project 4A161102AT24.
Bibliography: p. 10.
1. Acoustic emissions. 2. Fracture (mechanics). 3. Ice. 4. Plates. I. Chaplin, M. II. St. Lawrence, W.F. III. United States. Army. Corps of Engineers. IV. Army Cold Regions Research and Engineering Laboratory. V. Series: CRREL Report 81-6.

END

DATE
FILMED
10-81

DTIC